Journal of Membrane Science 655 (2022) 120584

Contents lists available at ScienceDirect

Journal of Membrane Science

journal homepage: www.elsevier.com/locate/memsci

Modification of polyamide reverse osmosis membranes for the separation of urea

Shahriar Habib, Steven T. Weinman *

Department of Chemical and Biological Engineering, The University of Alabama, Tuscaloosa, AL, 35487, USA

ARTICLE INFO

Keywords:
Thin-film composite membrane
Urea removal
Polyamide layer modification
Carbodiimide chemistry

ABSTRACT

Reverse osmosis (RO) membranes are the gold standard for water desalination and have been in use for over three decades. Even though RO membranes exhibit excellent performance rejecting monovalent and divalent salt ions, they do not reject small, neutral, and uncharged molecules, such as urea, to a level to produce potable water, especially at near-neutral pH. Due to the fast, uncontrolled nature of the interfacial polymerization reaction, the polyamide layer contains both network and aggregate free volume holes (pores). Because urea rejection is dominated by the size exclusion mechanism, reducing the free volume to reduce the passage of the urea through the membrane is needed. In this regard, the modification of RO membranes to increase the degree of cross-linking and/or decrease the free volume hole size is an ideal approach. We hypothesize that if the polyamide layer can be modified with a diamine, then the urea rejection will be increased. In this work, we modified polyamide RO membrane separation layers of commercial membranes (Dupont XLE and BW30XFR) using the carbodiimide chemistry followed by the application of m-phenylenediamine (MPD) and heat treatment in the post-modification stage. The modified membranes were characterized using ATR-FTIR, XPS, SEM, contact angle goniometry, and electrokinetic analyzer. Membranes were performance tested for water permeance, NaCl rejection, and urea rejection using a dead-end stirred cell. Compared to the control membranes, the modified XLE membranes and modified BW30XFR membranes improved the urea rejection from 16.8% to 54.9% and from 48.4% to 64.6%, but a reduction in water permeance by a factor of up to 4.7 and 2.7 respectively. The results show that combining the application of MPD and heat treatment can enhance the urea rejection of the membranes significantly.

1. Introduction

The scarcity of freshwater is becoming more prominent around the world day by day [1]. According to a United Nations report, by 2050, the global water demand will increase by 55%, and 40% of the global population will live in areas of serious water stress [2]. In conjunction with water stress, the exponential growth of the global population and the establishment of new chemical industries are polluting the freshwater sources [2–4]. The wastewater effluents produced by these municipalities and industries are rich in organic contaminants and often are not treated properly, resulting in the contamination of freshwater.

Although the existing water treatment technologies such as sedimentation, filtration, and coagulation are suitable to treat large organic contaminants, i.e., pesticides, small, neutral, uncharged organic molecules (SNUs) such as urea, boric acid, and N-nitrosodimethylamine (NDMA) are still hard to treat [5,6]. SNUs can be toxic and harm the environment [3,6–8], and thus need to be removed from water sources.

Recently, the urea concentration in freshwater and seawater sources has been increasing, leading to more attention by the scientific community to study how to remove it [3,9]. The presence of urea is primarily found in the effluent of the fertilizer industry, irrigation water from agriculture farms, and human waste [9,10]. An excessive amount of urea in irrigation water or freshwater is harmful to the human body and ecological stability [10,11]. For example, urea in wastewater can tremendously increase algae growth, which disturbs the ecological balance and releases ammonia that is toxic to fish [11].

To ensure the availability of potable and reusable water and maintain the sustainability of the environment, SNUs like urea must be treated effectively. There are numerous methods, such as hydrolysis, enzymatic hydrolysis, decomposition in a biological bed, decomposition by strong oxidants, adsorption, catalytic decomposition, and electrochemical oxidation, that are currently used for removing urea from

* Corresponding author.
E-mail address: stweinman@eng.ua.edu (S.T. Weinman).

https://doi.org/10.1016/j.memsci.2022.120584
Received 25 January 2022; Received in revised form 12 April 2022; Accepted 24 April 2022
Available online 27 April 2022

aqueous solutions [12]. However, most of these methods are either energy-intensive or require complex biological processes [13]. Moreover, some of these methods produce further waste via urea decomposition, making the treatment process more expensive and complex [14].

Recently, membrane separation techniques, such as forward osmosis (FO) and reverse osmosis (RO), have been studied to remove SNUs from water due to their simple operation and minimal requirement for the addition of chemicals during the treatment process [15]. However, in the case of FO membranes, the water recovery is quite low (25%) even though the urea rejection is above 82%, which is not feasible for many real-world water treatment applications [12]. In addition, the use of a draw solution and its recovery also increases the operational costs for FO processes [4]. RO is a mature technology for seawater desalination and has been studied for urea rejection [16]. RO is commonly used in desalination and water and wastewater treatment due to its outstanding performance in separating small monovalent ions via the size sieving and Donnan exclusion mechanisms [17]. Even though RO membranes exhibit excellent desalination performance, they do not reject SNUs at a high percentage (20–60%) [16,18–21]. The neutral charge of SNUs makes them significantly less impacted by the Donnan exclusion mechanism [18]. Therefore, reducing the free volume of the RO polyamide separation layer to reduce the passage of SNUs through the membrane is needed.

To improve SNU rejection, various approaches such as reducing the aggregated pores via heat treatment [22] or modification of surface via plugging [23] have been studied. In the study conducted by Fujioka et al., RO membrane performance for rejecting NDMA molecules was effectively enhanced by 46% via treating commercial membranes in a heated water bath [22]. In another study, Shultz et al. used aliphatic amines as molecular plugs to reduce the free volume pore size, which reduced the boron passage of the RO membrane by a factor of 2–4 [23]. To enhance the rejection of NDMA, Croll et al. used graphene oxide to modify the surface of a commercial RO membrane, which decreased the NDMA permeability coefficient by 31% [24]. Though a decent number of studies have been performed on increasing the rejection of SNUs, improving the RO membrane rejection of urea has not been well explored. To the best of our knowledge, there are still no polyamide RO membranes with a reported ability to remove urea greater than 64%.

The objective of this study was to enhance the urea rejection of polyamide RO membranes. We tested the hypothesis that modifying the carboxylic acid groups of commercial RO polyamide membranes with a secondary amine will increase the rejection of urea by altering the properties of the polyamide layer. In this work, we modified polyamide RO membrane separation layers of commercial membranes (Dupont XLE and BW30XFR) with m-phenylenediamine (MPD). We used carbodiimide chemistry to conjugate the MPD with free carboxylic acid groups present in the polyamide layer. The membrane chemical structure, hydrophilicity, and surface charge were analyzed before and after modification. The modified membranes were performance tested for water permeance, NaCl rejection, and urea rejection using a dead-end stirred cell.

2. Materials and methods

2.1. Materials

Crystallized urea (ACS grade, ≥ 99%), β-(N-Morpholino) ethanesulfonic acid buffer (MES, anhydrous, ≥99%), and 1-(3 Dimethylaminopropyl)-3-ethylcarbodiimide hydrochloride (EDC, ≥98%) were used as received from VWR. Sodium chloride (NaCl, ≥99%), m-Phenylenediamine (MPD, 99%), and 4-(2-Hydroxyethyl) piperazine-1-ethanesulfonic acid buffer (HEPES, ≥99.5%) were used as received from Sigma Aldrich (Millipore-Sigma). N-Hydroxysuccinimide (NHS, ≥98%) was used as received from TCI chemicals. Aqueous solutions were made with deionized water from a Millipore Synergy UV water purification system. Commercial polyamide thin-film composite reverse osmosis (RO) membranes (XLE and BW30XFR) were kindly provided by Dupont Water Solutions. These membranes consist of a polyester fabric backing, a polysulfone support layer, and a fully aromatic polyamide selective layer. The BW30XFR membrane has a coating on top of the polyamide layer while the XLE has no coating.

2.2. Membrane modification

The XLE and BW30XFR membranes were provided as flat sheet rolls and stored dry until use. Fig. 1 shows the schematic of the process used to modify the polyamide layer of the XLE and BW30XFR membranes. Before surface modification, each membrane was cut into circle coupons with an area of 19 cm^2 (a diameter of 4.92 cm^2) and immersed in DI water overnight. Then 0.77 g of EDC, 0.115 g of NHS, and 2.922 g of NaCl were weighed on a ME403E precision balance (Mettler Toledo) and put in a 250 mL beaker. Then, 100 mL of aqueous 10 mM MES buffer solution was added to the beaker and stirred. The pH of the solution was adjusted to 5 using 0.1 M HCl and 0.1 M NaOH. Next, the membrane coupon was put into the solution and placed on a VWR Standard Analog Shaker for 4 h for activation of the carboxylic acid groups on the polyamide layer. After activation, the membrane was put in a 250 mL beaker with (0 w/v% or 2 w/v%) MPD and 0.877 g NaCl in 100 mL of 10 mM HEPES buffer solution. The membrane was kept in the solution for 24 h at different temperatures (22 °C [room temperature], 47 °C (hot plate setting of 50 °C), 63 °C (hot plate setting of 80 °C), or 78 °C (hot plate setting of 95 °C)). To heat the solutions, a VWR hot plate integrated with a temperature indicator was used. The membranes will be discussed with the acronyms provided in Table 1 and Table 2. The control membranes are considered modified at 22 °C with no MPD. Note that we are not including any data for the EDC-NHS activated only membranes because the NHS half-life is on the order of minutes to hours depending on the physiological pH [25], and therefore, would not be a major factor in membrane property change.

2.3. Membrane characterization

2.3.1. ATR-FTIR

Attenuated total reflectance Fourier-transform infrared spectroscopy (ATR-FTIR) was used to characterize the surface chemistry of the control and modified XLE and BW30XFR membranes. The measurements were done using a Perkin Elmer Spectrum 2 ATR-FTIR spectrometer equipped with a diamond ATR crystal in the range of 400–4000 cm^{-1}. Data were processed by Spectrum 10 software. Each spectrum was collected for 32 scans at a resolution of 4 cm^{-1} and was baseline and ATR corrected with the Spectrum 10 software. All spectra were normalized to the peak at ~1490 cm^{-1}. A background of the ATR crystal was taken before each set of samples was tested to ensure the crystal was clean.

2.3.2. XPS

X-ray photoelectron spectroscopy (XPS) was used to analyze the elemental composition of the control and modified XLE and BW30XFR membranes. The XPS data were collected using a Phi Electronics Versaprobe 5000 with a monochromatic Al (1486.6 eV) micro-focused source (100 μm spot size). The survey scans were taken with a pass energy of 187.85 eV, step size of 0.8 eV, and 25 ms time per step. Eight scans were taken per sample and averaged. The scans were analyzed using the Phi Multipak software. The elemental composition was obtained using the software's automatic identification and background subtraction, and the ratio of the area under the peak for nitrogen and oxygen was used to determine the N/O ratio of the sample.

2.3.3. Static contact angle goniometry

Static water contact angles were measured on control and modified XLE and BW30XFR membrane samples to evaluate changes in hydrophilicity associated with the changes in surface chemistry. All static water contact angles were measured using the sessile drop method with

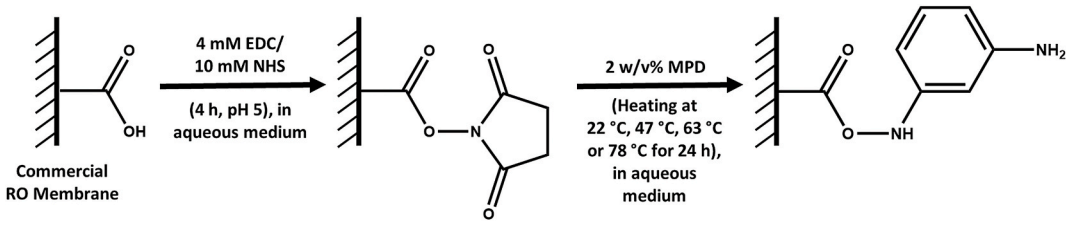

Fig. 1. Modification of polyamide layer reaction schematic. EDC/NHS is used to activate the carboxylic acid groups of the polyamide layer to allow for MPD coupling using heat.

Table 1
Acronyms for the XLE membranes.

Membranes	EDC/NHS	Modification Temperature	MPD
Control XLE (XLE-22)	Not used	22 °C	Not used
XLE-NHS-22-MPD	Used	22 °C	Used
XLE-NHS-47-MPD	Used	47 °C	Used
XLE-NHS-63-MPD	Used	63 °C	Used
XLE-NHS-78-MPD	Used	78 °C	Used
XLE-47	Not used	47 °C	Not used
XLE-63	Not used	63 °C	Not used
XLE-78	Not used	78 °C	Not used

Table 2
Acronyms for the BW30XFR membranes.

Membranes	EDC/NHS	Modification Temperature	MPD
Control BW30 (BW30-22)	Not used	22 °C	Not used
BW30-NHS-22-MPD	Used	22 °C	Used
BW30-NHS-47-MPD	Used	47 °C	Used
BW30-NHS-63-MPD	Used	63 °C	Used
BW30-NHS-78-MPD	Used	78 °C	Used
BW30-47	Not used	47 °C	Not used
BW30-63	Not used	63 °C	Not used
BW30-78	Not used	78 °C	Not used

a Dataphysics OCA-15EC contact angle analyzer. A liquid drop of deionized water (~15 μL) was placed carefully on the sample surface. The sessile drop model was used in SCA 20 Analysis software to determine each contact angle. For consistency, measurements were taken 70 s after each water droplet was placed on the surface. Measurements were done at a minimum of three locations on each sample to get an average contact angle value with standard deviation.

2.3.4. Streaming potential analysis

The zeta potential of the control and modified XLE and BW30XFR membrane surfaces were determined using an electrokinetic analyzer (SurPASS 3, Anton-Paar). Two membrane coupons were fixed to the sample holders of an adjustable gap cell with a gap size of 100 μm (sample size is 20 mm × 10 mm). In the experiment, an aqueous 0.01 M KCl solution was used as the measuring solution. For the pH adjustment, 0.05 M HCl and 0.05 M NaOH were used. The zeta potential was measured sequentially at pH 6, 9, and 3. The zeta potential was computed using the SurPASS 3 software using the Helmholtz-Smoluchowski equation. Measurements were done a minimum of three times to get an average zeta potential value with standard deviation.

2.4. Membrane testing

The water permeance, NaCl rejection, and urea rejection of the control and modified XLE and BW30XFR membranes were measured using a Sterlitech HP4750 dead-end stirred filtration cell (Sterlitech, USA) with a cell volume of 270 mL and an effective filtration area of 14.6 cm^2. The filtration cell was pressurized with nitrogen gas to a pressure of 230 psi. Each membrane was challenged with a DI water solution, a 2000 ppm NaCl solution, and a 500 ppm urea solution. Each membrane was allowed to permeate for 30 min to allow for compaction before the permeate was collected on a ME403E precision balance (Mettler Toledo). At least 8 g of permeate was collected while recording the time to calculate the flux through the membrane. At least 3 membranes were tested for each membrane type for statistical relevance. The NaCl rejection was calculated by measuring the conductivity of the feed and permeate solutions using a VWR Traceable Bench/Portable Conductivity Meter. The urea rejection was calculated by measuring the urea concentration of the feed and permeate using a HACH DR6000 UV-VIS Laboratory Spectrophotometer at 195 nm wavelength using quartz cuvettes (VWR), similar to Cheah and coworkers [1]. A calibration curve was constructed to calculate the urea concentration. Each sample was diluted two times using DI water because the calibration curve started to deviate from linear above 400 ppm. The rejection of NaCl and urea were calculated using Equation (1):

$$R = C_p/C_f \quad (1)$$

where C_p and C_f are the permeate and feed concentrations, with the calibration curve for NaCl and urea concentrations shown in Figs. S1A and S1B.

The standard flux and permeance model described by Equation (2) was used to calculate the water permeance of each experiment

$$J_w = A\ (\Delta P\text{-}\Delta\pi) \quad (2)$$

where J_w is the flux (L/m^2/h or LMH) of the permeate solution, A is the membrane permeance (LMH/bar), ΔP is the difference in pressure (bar) between the feed and permeate (atmospheric pressure, 0 barg), and Δπ is the difference in osmotic pressure (bar) between the retentate and permeate. The osmotic pressure of each solution was calculated using Equation (3):

$$\pi = iCRT \quad (3)$$

Where i is the dissociation constant (2 for NaCl and 1 for urea), C is the concentration of NaCl or urea (mol/L), R is the universal gas constant (0.08314 L*bar/(mol*K)), T is the testing solution temperature (295 K).

The flux of each membrane was calculated by dividing the permeate flow rate by the membrane testable area. For deionized water experiments, the flux was divided by the pressure difference (ΔP) to calculate the pure water permeance. For salt and urea rejection experiments, the flux was divided by (ΔP−Δπ) to calculate the water permeance.

The solute permeability for both NaCl and urea was calculated for each pressure and trial using Equation (4).

$$J_s = J_w \times C_p \quad (4)$$

where J_s is the solute flux (mol/(m^2*h)), J_w is the calculated water flux (LMH), and C_p is the solute concentration of the permeate solution (mol/L).

3. Result and discussion

3.1. Membrane characterization

The commercial membranes were post-modified using MPD. To conjugate MPD with the polyamide layer, EDC was used to activate the free carboxylic acid groups of the polyamide layer. EDC reacts with the carboxylic acid groups and forms an unstable O-acylisourea intermediate [26]. To form a more stable intermediate, NHS was used [26]. The EDC couples the carboxyl acid groups with NHS and forms a dry-stable NHS-ester intermediate [26]. Lastly, the NHS-ester intermediate couples the carboxyl acid groups with MPD, forming a new polyamide bond, which was confirmed by the ATR-FTIR and XPS data. Fig. 2A shows the ATR-FTIR spectra of the control and modified XLE membranes. Each membrane showed characteristic peaks at ~1660 cm^{-1}, ~1610 cm^{-1}, and ~1540 cm^{-1}, representing the amide I band, aromatic amide band, and amide II band of a fully aromatic polyamide layer [27]. Membranes modified using MPD did not exhibit any shifts or changes in peak position compared to the control. However, the MPD modified membranes showed a slightly more intense amide I band peak, a more intense aromatic amide band peak, and a more intense amide II bond peak. When the heat was introduced along with employing the MPD to the modification process, the peak intensity was found to be increased further. We suspect the addition of heat increased the rate of reaction between MPD and activated carboxylic groups, causing more MPD molecules to react to the membrane surface. However, the peak intensity did not increase monotonically with an increase in the modification temperature, indicating the reaction rate on the membrane surface does not increase linearly with temperature. Fig. 2B shows the ATR-FTIR spectra of control and modified BW30XFR membranes. Similar to the control and modified XLE membranes, the BW30XFR membranes also showed the key peaks at the same wavelengths and an increase in the peak intensity was observed with the extent of modification. To understand the effect of MPD on the modification at high temperatures, both the XLE and BW30XFR membranes were modified at 47 °C, 63 °C, and 78 °C without using MPD, and in both cases, the peak intensity was found to be similar compared to the controls (Fig. S2 in the Supporting Data). Thus, the increase in the intensity of these peaks indicated the presence of more amide groups on the polyamide separation layer, which mostly happened due to the introduction of MPD.

The control and modified XLE and BW30XFR membranes were further characterized by XPS. Table 3 shows the data obtained from the XPS characterization. As each MPD molecule possesses two nitrogen atoms and no oxygen atoms, the membranes after modification should have a larger nitrogen-to-oxygen (N/O) ratio than the control membranes, because one oxygen atom is removed for the addition of two nitrogen atoms. The amount of MPD added to the membrane surfaces is unlikely to significantly change the amount of C present in the whole polyamide layer thickness measured by XPS, which is seen in Table 3. We are only modifying the membrane surfaces; it is highly unlikely that the EDC-NHS activators penetrate the crosslinked polyamide layers. Compared to the control XLE membranes, the N/O ratio of modified XLE membranes had a statistical increase when the modification was done using MPD at room temperature (statistical analysis shown in Table S1 of the Supporting Data). The N/O ratio increased with an increase of the modification temperature indicating more MPD on the polyamide layer. In the case of BW30XFR membranes, the N/O ratio of BW30-NHS-22-MPD, BW30-NHS-47-MPD, BW30-NHS-63-MPD, and BW30-NHS-78-MPD did not change statistically (Table S1) compared to the control. The extent of MPD modification was not very apparent due to the more crosslinked and tighter network structure of BW30XFR membranes. However, the average values for the BW30-NHS-63-MPD and BW30-NHS-78-MPD membranes were higher than the control BW30XFR membrane, just with a larger variance, suggesting more modification with MPD happened at 63 °C and 78 °C.

Table 3
XPS data of the control and modified XLE and BW30XFR membranes. The error represents one standard deviation among three membrane samples.

Membrane	C	N	O	N/O Ratio
Control XLE	74.84 ± 0.53	10.77 ± 0.63	14.39 ± 0.23	0.75 ± 0.05
XLE-NHS-22-MPD	73.94 ± 0.49	14.16 ± 0.58	11.90 ± 0.15	1.19 ± 0.06
XLE-NHS-47-MPD	73.10 ± 1.31	14.53 ± 0.78	12.38 ± 1.09	1.18 ± 0.12
XLE-NHS-63-MPD	74.60 ± 1.74	14.86 ± 0.77	10.54 ± 1.28	1.42 ± 0.15
XLE-NHS-78-MPD	73.97 ± 1.82	15.61 ± 1.07	10.42 ± 0.86	1.50 ± 0.07
Control BW30	73.70 ± 0.40	12.88 ± 0.36	13.42 ± 0.77	0.96 ± 0.08
BW30-NHS-22-MPD	74.75 ± 0.08	12.58 ± 0.16	12.68 ± 0.08	0.99 ± 0.02
BW30-NHS-47-MPD	73.53 ± 1.47	12.93 ± 1.01	13.54 ± 1.41	0.96 ± 0.15
BW30-NHS-63-MPD	72.60 ± 1.18	14.96 ± 0.93	12.43 ± 1.68	1.22 ± 0.20
BW30-NHS-78-MPD	71.94 ± 2.93	14.77 ± 1.39	13.30 ± 2.85	1.16 ± 0.30

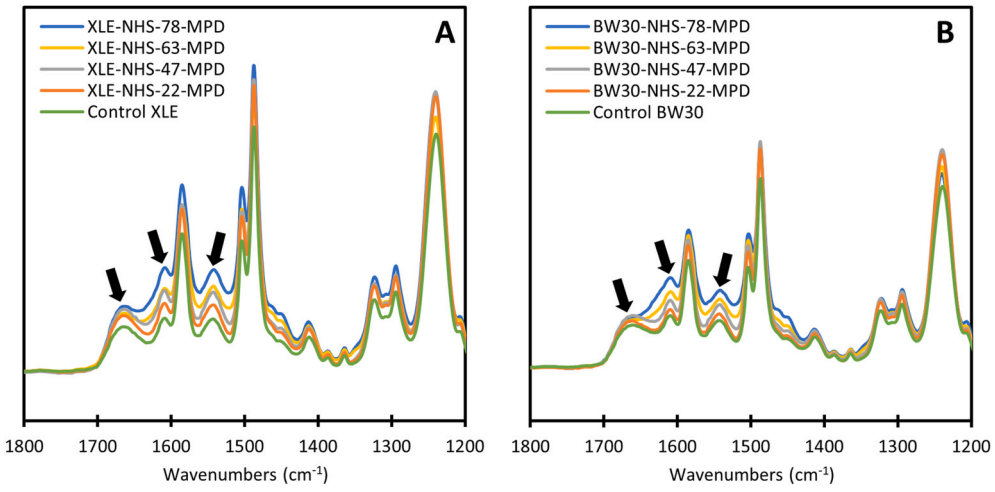

Fig. 2. ATR-FTIR spectra of (A) control XLE membrane and XLE membrane modified with 2% MPD at 22 °C, 47 °C, 63 °C, and 78 °C, and (B) control BW30XFR membrane and BW30XFR membrane modified with 2% MPD at 22 °C, 47 °C, 63 °C, and 78 °C.

To determine whether the surface morphology changed with temperature and/or MPD modification, SEM imaging of the XLE and BW30XFR membranes was performed for both control and modified membranes. The SEM images are presented in Fig. S3 (XLE) and Fig. S4 (BW30XFR). The surface morphology was found to be the same for all membranes. Both control and modified membranes exhibited ridge-and-valley structure with no apparent change. Even if any changes have occurred, it likely happened at the angstrom-scale, which requires advanced characterization techniques like positron annihilation lifetime spectroscopy (PALS) to detect.

To understand the effect of the modification on the hydrophobicity of the XLE and BW30XFR membranes, static water contact angle measurements were performed. Fig. 3A and B shows the water contact angle data for the XLE and BW30XFR membranes. Compared to the control XLE and BW30XFR membranes, the MPD modified membranes exhibited a statistical increase in water contact angle, which indicates an increased hydrophobicity of the polyamide layer (statistical analysis shown in Table S2 of the Supporting Data). The increase in the water contact angle is believed to happen due to the binding of MPD to the NHS-activated surface, which decreased the amount of hydrophilic carboxylic acid moieties and increased the amount of hydrophobic aromatic rings. We suspect that with more MPD attachment, there will be more amine-water hydrophilic interactions and less aromatic ring-water hydrophobic interactions, keeping the water contact angle approximately the same for the all the XLE and BW30XFR MPD-modified membranes.

To investigate the effect of MPD modification on membrane surface charge, the zeta potential of each membrane was measured at pH 9, 6, and 3, as shown in Fig. 4A and B. The surface charge of the control and modified XLE membranes were positive at pH 3. The XLE membrane modified with MPD at all temperatures exhibited a higher positive surface charge at pH 3 than the control XLE membrane. In the case of pH 6, all the XLE membranes showed a negative surface charge, with the control XLE membrane showing the most negative surface charge, and the XLE membrane modified at 78 °C with MPD showing the least negative surface charge. The zeta potential of the modified XLE membranes also was found to be increased at pH 9 compared to the control XLE membrane. The phenomenon of less negative surface charge for modified XLE membranes at pH 9 can be attributed to the increased positive charge density of the protonated amine groups from the newly incorporated MPD molecules and a decrease in the deprotonated carboxylic acid groups.

Similar to XLE membranes, the zeta potential of the modified BW30XFR membranes exhibited a higher positive surface charge compared to the control BW30XFR at pH 3. The modified BW30XFR membranes also showed an increase in zeta potential value with increasing modification temperatures at pH 6. For the zeta potential values at pH 9, except for the BW30-NHS-22-MPD membrane, all the modified BW30XFR membranes showed a higher zeta potential than the control membrane.

When we compared the zeta potential of Control XLE, XLE-47, XLE-63, and XLE-78, we observed a similar or slight change in zeta potential at pH 3, pH 6, and pH 9 (See Fig. S5A in the Supporting Data). In the case of the BW30XFR membranes (See Fig. S5B in the Supporting Data), Control BW30, BW30-47, BW30-NHS-63, and BW30-78 membranes exhibited similar or slight change in zeta potential at pH 3, pH 6, and pH 9.

3.2. Membrane performance

Membrane performance including, pure water permeance, NaCl rejection, and urea rejection were measured for both XLE and BW30XFR membranes. Fig. 5 shows the pure water permeance results for the XLE and BW30XFR membranes. For both XLE and BW30XFR membranes, the modified membranes exhibited a statistical decrease in pure water permeance compared to their respective control membranes with the increase in the modification temperature (see Table S3 in the supporting data). This may be attributed to the reduction in the free volume due to the increased coupling of MPD and/or rearrangement of the pores due to heat treatment.

Fig. 6 shows the membrane performance results for the XLE membranes when challenged with NaCl and urea solutions. Fig. 6A show the water permeance and NaCl rejection for the control and modified XLE membranes. As the experiment was performed using a dead-end stirred cell setup and some extent of concentration polarization possibly happened [28], the NaCl rejection of all the XLE membranes was lower than the manufacturer's provided value (97%), where a crossflow setup was used. Paired t-tests were done to compare the results of water permeance (see Table S4 in the Supporting Data) and NaCl rejection (see Table S5 in the Supporting Data) for the control XLE and modified XLE membranes. The NaCl rejection of the membranes modified with MPD at room temperature (22 °C) and 47 °C were found to be statistically similar to the control XLE. In case of the XLE membranes, which were modified only using heat exhibited similar NaCl rejection compared to the control membrane. However, in the case of XLE-NHS-63-MPD and XLE-NHS-78-MPD, the NaCl rejection had a statistical decrease. Also,

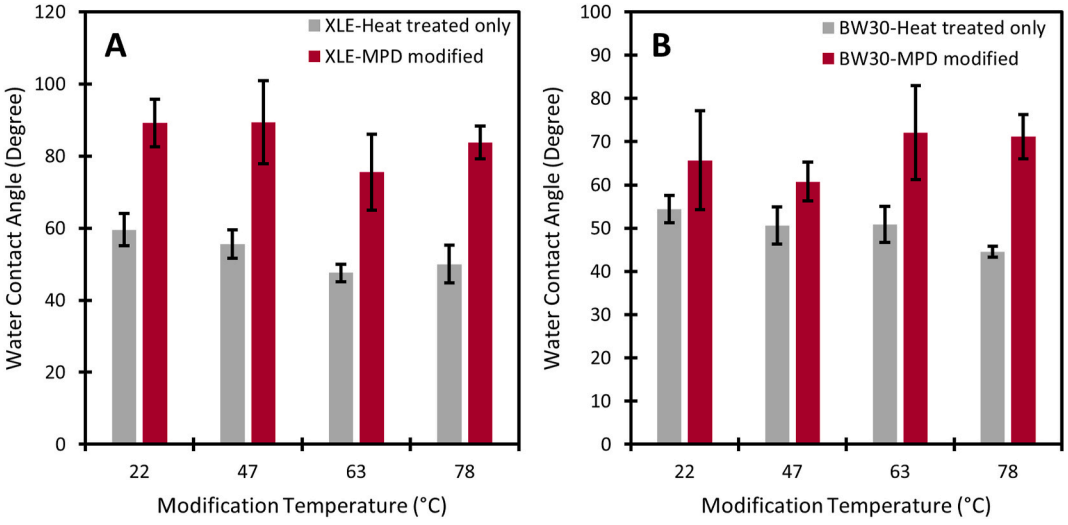

Fig. 3. Water contact angle of (A) control XLE and modified XLE membranes and (B) control BW30 and modified BW30 membranes. The error bars represent one standard deviation among at least three data points.

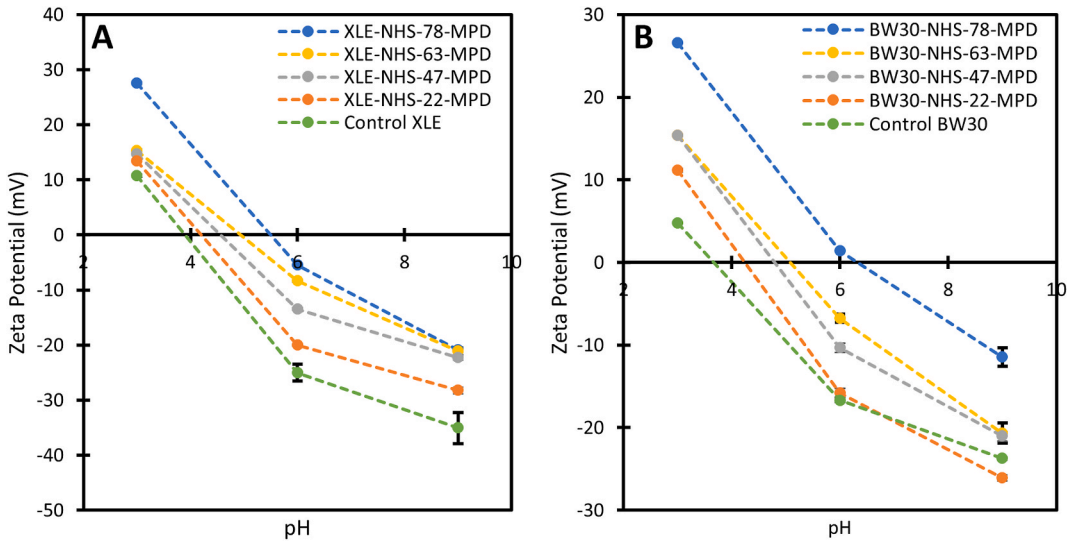

Fig. 4. Zeta potential of (A) control XLE membrane and XLE membrane modified with 2% MPD at 22 °C, 47 °C, 63 °C, and 78 °C, and (B) control BW30XFR membrane and BW30XFR membrane modified with 2% MPD at 22 °C, 47 °C, 63 °C, and 78 °C at pH 3, pH 6 and pH 9. The error bars represent one standard deviation among three tests. The dashed lines between data points are included to aid in the visual comparison of the different modifications.

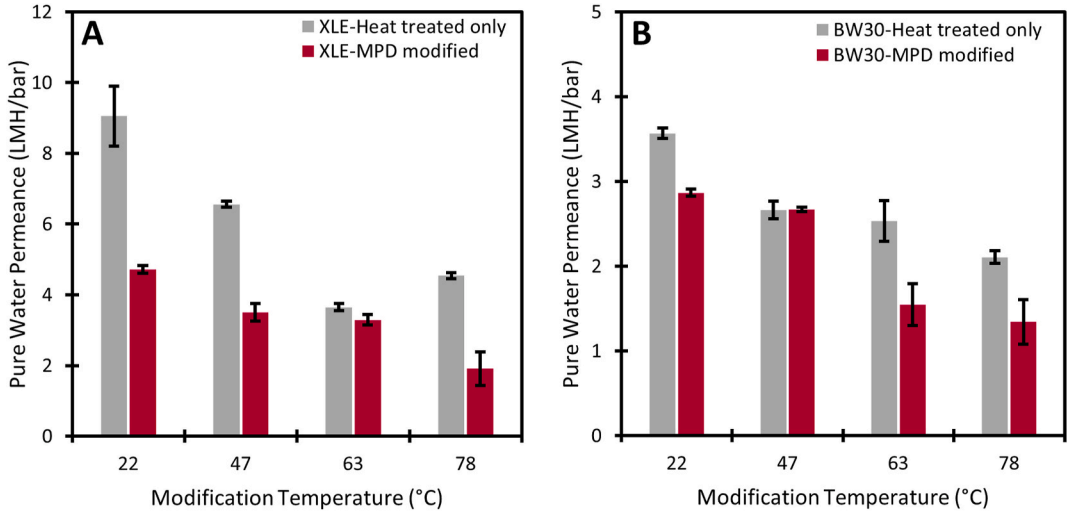

Fig. 5. Pure water permeance of (A) control XLE and modified XLE membranes and (B) control BW30 and modified BW30 membranes. The error bars represent one standard deviation among three membrane samples.

the NaCl rejection for the XLE-NHS-63-MPD and XLE-NHS-78-MPD membranes were statistically different from their heat-modified counterparts. The decrease in the NaCl rejection at higher temperatures can be explained by the reduction of the Donnan charge exclusion effect [29]. At higher temperatures, more MPD molecules reacted with the activated carboxylic acid groups, forming a polyamide bond, and reducing the available negatively charged moieties to reject the chloride ions of NaCl. The decrease in the negative charge, and likely the free volume, of the polyamide layer also affected the water permeance of the XLE membranes. The control XLE membrane had an average water permeance of 7.95 ± 0.57 L/m^2/h/bar. All of the modified XLE membranes had a statistical decrease in water permeance compared to the control XLE membrane. XLE membranes modified using MPD at 22 °C, 47 °C, 63 °C and 78 °C had an average water permeance of 5.30 ± 0.19, 4.20 ± 0.16, 3.46 ± 0.01 and 1.98 ± 0.42 L/m^2/h/bar respectively. For the heat-treated membranes, their water permeance values were lower than the control XLE membrane but higher than their MPD-modified counterparts. Compared to the control XLE membrane, the MPD-modified XLE membranes exhibited lower water permeance likely due to the tighter structure, pore rearrangement, and increased hydrophobicity and the heat-treated XLE membranes exhibited lower water permeance likely due to pore rearrangement.

Fig. 6B show the water permeance and urea rejection of the control XLE and modified XLE membranes. Similar to the NaCl rejection tests, the water permeance had a statistical decrease with an increase in the modification temperature (see Table S6 in the Supporting Data). In the case of urea rejection for the XLE membranes, the urea rejection was found to be increased from 16.8% to 36.3% when the XLE membrane was modified with MPD at room temperature (22 °C) compared to the control XLE membrane (see Table S7 in the Supporting Data). Unlike the NaCl rejection, the modified XLE membranes showed a continuous increase of urea rejection with increasing modification temperature. The urea rejection of XLE-NHS-47-MPD, XLE-NHS-63-MPD, and XLE-NHS-78-MPD membranes had a statistical increase up to 46.3%, 54.4%, and 54.9% respectively when compared with control XLE. The increase in urea rejection at high temperature is likely attributed to the reduction of the free volume of the polyamide layer by both MPD attachment and pore rearrangement from the hot water bath.

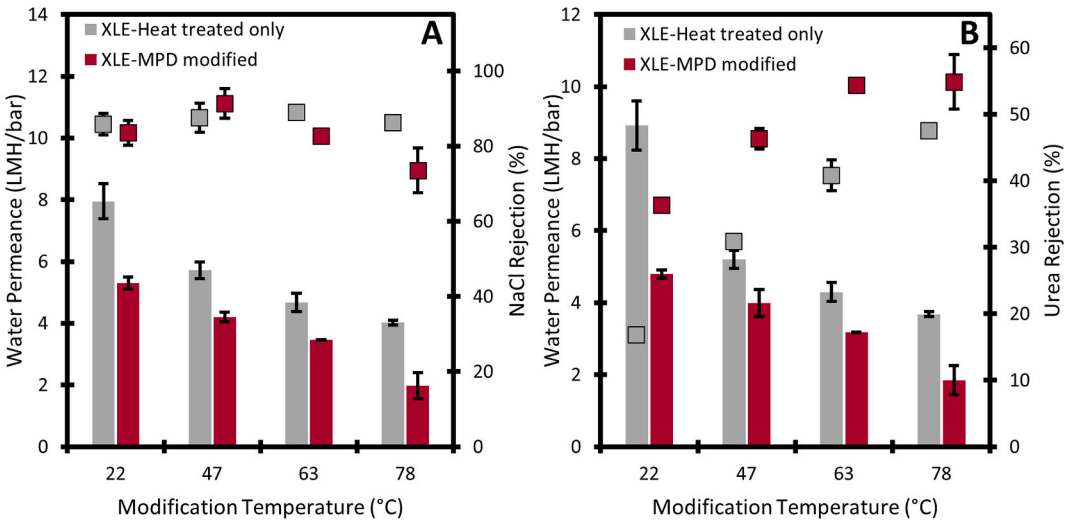

Fig. 6. (A) Water permeance and NaCl rejection of control XLE and modified XLE membranes, and (B) water permeance and urea rejection of control XLE and modified XLE membranes. The columns represent the water permeance data and the black outlined squares represent the NaCl (A) or urea (B) rejection data. The error bars represent one standard deviation among three membrane samples.

Fig. 7 represents the membrane performance data of the BW30XFR membranes when challenged with NaCl and urea solutions. Fig. 7A show the water permeance and NaCl rejection for the control and modified BW30XFR membranes respectively. The BW30XFR NaCl rejection was found to follow the same trend exhibited by the XLE membranes. Modifying the BW30XFR membranes at room temperature (22 °C) did not change the NaCl rejection statistically compared to the control BW30 membrane (see Table S5 in the Supporting Data). But, when the modification temperature was 63 °C and 78 °C, the NaCl rejection had a statistical decrease. There was a statistical increase in the urea rejection and decrease in water permeance when the modification temperature of BW30XFR membrane was increased, which is shown in Fig. 7B (see Tables S6 and S7 in the Supporting Data). Compared to the control BW30XFR, the urea rejection of BW30-NHS-22-MPD, BW30-NHS-47-MPD, BW30-NHS-63-MPD, and BW30-NHS-78-MPD were increased up to 54.1%, 56.6%, 59.4%, and 61.3% respectively. However, the magnitude of the change in urea rejection between the control BW30XFR and the modified BW30XFR membranes was smaller than the change between the control XLE and the modified XLE membranes. This can be explained by the presence of a more crosslinked polyamide layer of BW30XFR membrane compared to the less crosslinked polyamide layer of the XLE membrane [30].

To understand the role of heat treatment in the modification and its effect on the urea rejection, both the XLE and BW30XFR membranes were modified at 22 °C, 47 °C, 63 °C, and 78 °C using 0% MPD. In the case of the XLE membranes, when XLE-NHS-22-MPD and control XLE (which we considered as XLE-22) were compared, the urea rejection was found to be statistically increased for the XLE-NHS-22-MPD, which is shown in Fig. 6B. Similarly, the presence of MPD increased the urea rejection of the XLE-NHS-47-MPD, XLE-NHS-63-MPD, and XLE-NHS-78-MPD membranes when compared to their heat-treated counterparts, XLE-47, XLE-63, and XLE-78. However, the urea rejection of the modified XLE membrane using 0% MPD at 47 °C, 63 °C, and 78 °C had a statistical increase compared to the control XLE membrane. This indicates not only MPD but also heat played an important role in improving the urea rejection of XLE membranes [22].

The BW30XFR membranes modified with 2% MPD at 22 °C exhibited improved urea rejection compared to the control BW30XFR membrane,

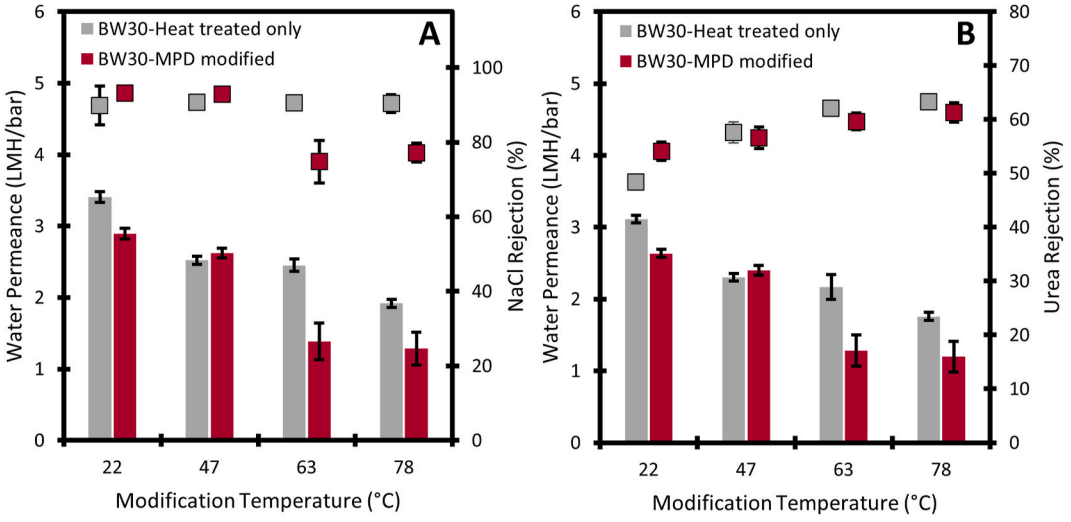

Fig. 7. (A) Water permeance and NaCl rejection of control BW30XFR and modified BW30XFR membranes, and (B) water permeance and urea rejection of control BW30XFR and modified BW30XFR membranes. The columns represent the water permeance data and the black outlined squares represent the NaCl (A) or urea (B) rejection data. The error bars represent one standard deviation among three membrane samples.

which is shown in Fig. 7B. Interestingly, when we compared the BW30-NHS-47-MPD, BW30-NHS-63-MPD and BW30-NHS-78-MPD membranes with BW30-47, BW30-63 and BW30-78, we have observed similar urea rejection. When the modification temperature was at 47 °C or higher, the heat played a more crucial role than the MPD. Because of the application of heat, it is likely the pores were narrowed, which decreased the free volume of the polyamide layer and increased the urea rejection [22]. On the other hand, as the polyamide layer of the BW30XFR membrane is denser and had a lower number of free carboxylic acid groups available, the MPD failed to contribute to a great extent to the improved urea rejection. The commercial coating on the polyamide layer of the BW30XFR membrane also may play a crucial role in preventing the MPD from modifying the polyamide layer significantly. However, the BW30XFR membranes modified without MPD at different temperatures showed higher water permeance compared to the BW30XFR membranes modified using MPD. Even though there was an increase in the urea rejection for the MPD modified XLE and BW30XFR membranes, a 1.9–4.7-fold and a 1.2–2.7-fold decrease in pure water permeance was observed compared to the control XLE and BW30XFR membranes.

Lastly, we calculated the NaCl and urea solute permeability to get a better understanding of the solute transport through the membrane. Fig. 8A–D shows the results. When we compared the NaCl solute permeability of the control XLE and XLE-NHS-22-MPD, we observed a higher NaCl solute permeability for the control XLE membrane. At higher temperatures, the membranes showed similar NaCl solute permeability regardless of whether MPD was used or not. In the case of control BW30 and modified BW30 membranes, the NaCl solute permeabilities were statistically the same. Even though, the XLE and BW30 membranes that were modified with MPD at higher temperatures (63 °C and 78 °C) showed lower water permeance which could decrease the NaCl solute permeability, the lower NaCl rejection of these membranes is likely due to the absence of repulsion charges from the carboxylic acid groups increased the NaCl permeability.

However, urea solute permeability was statistically decreased when the XLE membranes were modified with MPD at 22 °C, 47 °C, 63 °C, and 78 °C. The heat-treated XLE membranes showed higher urea solute permeability compared to their MPD-modified counterparts, but lower than the control XLE membrane. We suspect the mechanism for improved urea rejection with heat treatment is due to the thermal rearrangement of the polyamide layer, which needs to be investigated with PALS measurements. The combination of a higher water flux and lower urea rejection for the heat-treated membranes lead to this significant difference in urea solute permeability. In the case of BW30

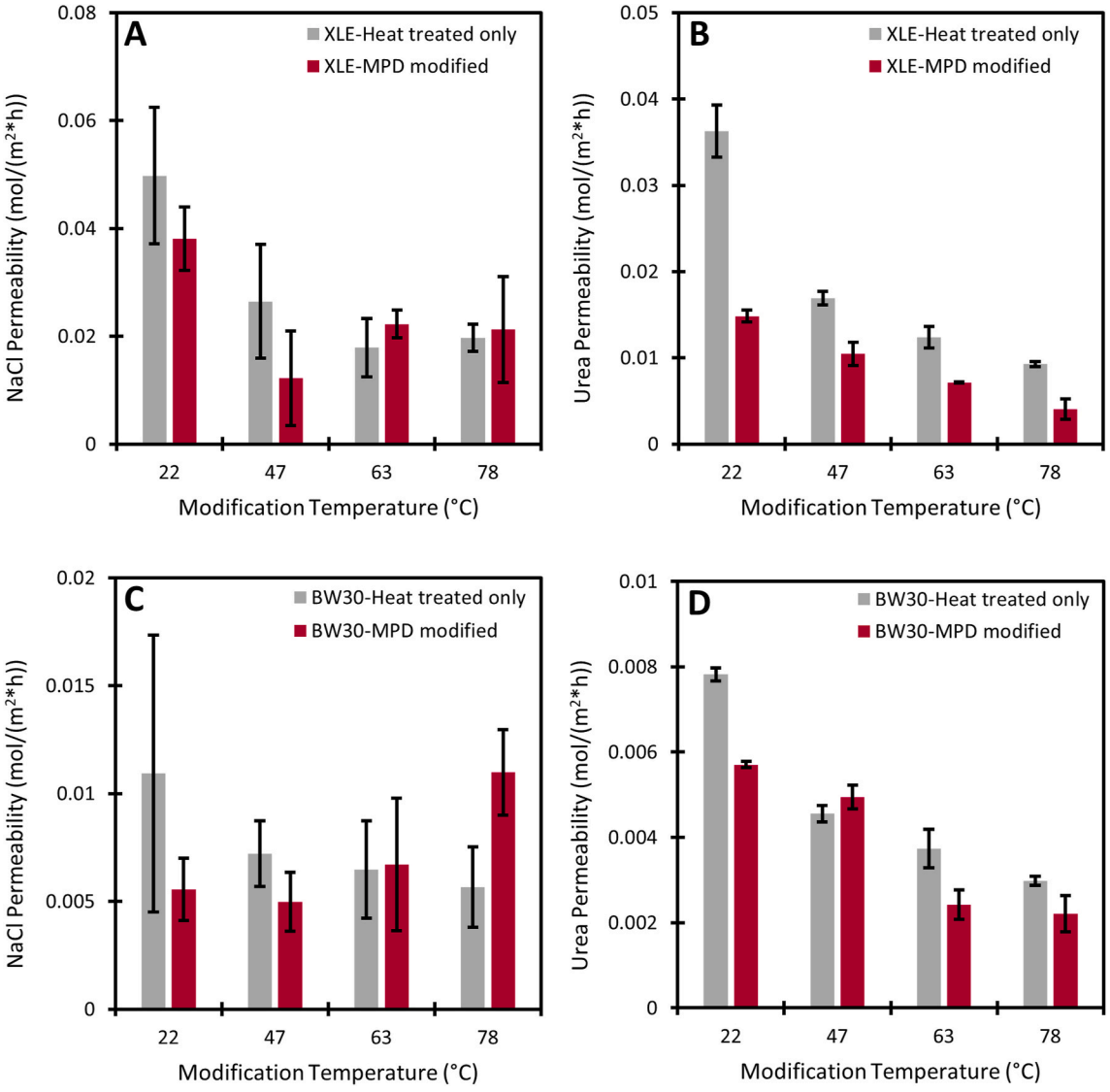

Fig. 8. (A) NaCl solute permeability and (B) urea solute permeability of control XLE and modified XLE membranes, and (C) NaCl solute permeability and (D) urea solute permeability of control BW30XFR and modified BW30 membranes. The error bars represent one standard deviation among three membrane samples.

membranes, except the BW30-47 membrane, the urea solute permeability was higher for the heat-treated only membranes compared to their MPD-modified counterparts. The BW30-NHS-47-MPD membrane and the BW30-47 membrane showed similar urea solute permeability, as both showed almost same water permeance and urea rejection.

4. Conclusion

A method was developed for combining chemical modification and heat treatment of commercial XLE and BW30XFR membranes to enhance the rejection of urea. For the chemical modification, carbodiimide chemistry was used followed by the coupling of MPD. The chemical modification of the commercial membranes was performed at room temperature (~22 °C) and higher temperatures (47 °C–78 °C). Whereas the control XLE and BW30XFR membranes had an average urea rejection of 16.8% and 48.4% respectively, the modified XLE and BW30 membranes had a 36.3–54.9% and 54.1–64.6% urea rejection depending on the modification temperature and percentage of MPD applied during the post-modification. These results supported our hypothesis. The increase in urea rejection of the modified XLE membranes was attributed mainly to the employment of MPD in the post-modification stage, whereas the increase in urea rejection for the modified BW30XFR membranes was attributed to the hot water bath treatment. However, in the case of both membranes, the water permeance was reduced significantly, although this is to be expected if the free volume hole size is reduced. Ongoing work is exploring alternative chemical modification strategies, including more investigation into the effect of heat treatment, to further increase the urea rejection and water permeance and quantifying the free volume hole size change through PALS measurements.

Author statement

Shahriar Habib: Conceptualization, Data curation, Formal analysis Investigation, Methodology, Validation, Visualization. Writing - original draft, Writing - review & editing. **Steven T. Weinman:** Conceptualization, Formal analysis, Funding acquisition, Methodology, Project administration, Supervision, Validation, Visualization, Writing - review & editing.

Declaration of competing interest

The authors declare that they have no known competing financial interests or personal relationships that could have appeared to influence the work reported in this paper.

Acknowledgement

The authors would like to acknowledge the financial support of the Department of the Interior (DOI), Bureau of Reclamation (BR) under agreement number R19AC00087. We thank the National Science Foundation (NSF) under award number CBET-1941700 and the Alabama Water Institute for their financial support to purchase the Anton Paar SurPASS 3. Any opinions, findings, conclusions, and/or recommendations expressed in this material are those of the authors(s) and do not necessarily reflect the views of the DOI, BR or NSF. We thank Dr. Caleb Funk for kindly providing the membranes used in this study. We thank Dr. Jason Bara for the use of his ATR-FTIR instrument.

Appendix A. Supplementary data

Supplementary data to this article can be found online at https://doi.org/10.1016/j.memsci.2022.120584.

References

[1] C.J. Vörösmarty, P. Green, J. Salisbury, R.B. Lammers, Global water resources: vulnerability from climate change and population growth, Science 289 (2000) 284–288.
[2] U. Water, The United Nations World Water Development Report 2014: Water and Energy, United Nations, Paris, 2014.
[3] S. Gopi, A.M. Al-Mohaimeed, M.S. Elshikh, K. Yun, Facile fabrication of bifunctional SnO–NiO heteromixture for efficient electrocatalytic urea and water oxidation in urea-rich waste water, Environ. Res. 201 (2021) 111589.
[4] A. Aende, J. Gardy, A. Hassanpour, Seawater desalination: a review of forward osmosis technique, its challenges, and future prospects, Processes 8 (2020) 901.
[5] Y. Kiso, Y. Sugiura, T. Kitao, K. Nishimura, Effects of hydrophobicity and molecular size on rejection of aromatic pesticides with nanofiltration membranes, J. Membr. Sci. 192 (2001) 1–10.
[6] J. Yang, Z. Shen, J. He, Y. Li, Efficient separation of small organic contaminants in water using functionalized nanoporous graphene membranes: insights from molecular dynamics simulations, J. Membr. Sci. 630 (2021) 119331.
[7] I. Uluisik, H.C. Karakaya, A. Koc, The importance of boron in biological systems, J. Trace Elem. Med. Biol. 45 (2018) 156–162.
[8] R. Bernstein, S. Belfer, V. Freger, Toward improved boron removal in RO by membrane modification: feasibility and challenges, Environ. Sci. Technol. 45 (2011) 3613–3620.
[9] Y. Chen, H. Chen, Z. Chen, H. Hu, C. Deng, X. Wang, The benefits of autotrophic nitrogen removal from high concentration of urea wastewater through a process of urea hydrolysis and partial nitritation in sequencing batch reactor, J. Environ. Manag. 292 (2021) 112762.
[10] H. Han, R. Gao, Y. Cui, S. Gu, Transport and transformation of water and nitrogen under different irrigation modes and urea application regimes in paddy fields, Agric. Water Manag. 255 (2021) 107024.
[11] M. Rahimpour, M. Barmaki, H. Mottaghi, A comparative study for simultaneous removal of urea, ammonia and carbon dioxide from industrial wastewater using a thermal hydrolyser, Chem. Eng. J. 164 (2010) 155–167.
[12] S. Engelhardt, J. Vogel, S.E. Duirk, F.B. Moore, H.A. Barton, Urea and ammonium rejection by an aquaporin-based hollow fiber membrane, J. Water Proc. Eng. 32 (2019) 100903.
[13] E. Urbańczyk, M. Sowa, W. Simka, Urea removal from aqueous solutions—a review, J. Appl. Electrochem. 46 (2016) 1011–1029.
[14] A. Zaher, N. Shehata, Recent advances and challenges in management of urea wastewater: a mini review, in: IOP Conference Series: Materials Science and Engineering, IOP Publishing, 2021, 012021.
[15] W. Hirunpinyopas, E. Prestat, S.D. Worrall, S.J. Haigh, R.A. Dryfe, M.A. Bissett, Desalination and nanofiltration through functionalized laminar MoS2 membranes, ACS Nano 11 (2017) 11082–11090.
[16] H. Ray, F. Perreault, T.H. Boyer, Rejection of nitrogen species in real fresh and hydrolyzed human urine by reverse osmosis and nanofiltration, J. Environ. Chem. Eng. 8 (2020) 103993.
[17] L.F. Greenlee, D.F. Lawler, B.D. Freeman, B. Marrot, P. Moulin, Reverse osmosis desalination: water sources, technology, and today's challenges, Water Res. 43 (2009) 2317–2348.
[18] K.L. Tu, L.D. Nghiem, A.R. Chivas, Boron removal by reverse osmosis membranes in seawater desalination applications, Separ. Purif. Technol. 75 (2010) 87–101.
[19] H. Ozaki, H. Li, Rejection of organic compounds by ultra-low pressure reverse osmosis membrane, Water Res. 36 (2002) 123–130.
[20] Y. Yoon, R.M. Lueptow, Removal of organic contaminants by RO and NF membranes, J. Membr. Sci. 261 (2005) 76–86.
[21] X. Zhang, Y. Yang, H.H. Ngo, W. Guo, H. Wen, X. Wang, J. Zhang, T. Long, A critical review on challenges and trend of ultrapure water production process, Sci. Total Environ. 785 (2021) 147254.
[22] T. Fujioka, M. Osako, K. Oda, T. Shintani, H. Kodamatani, Impact of heat modification conditions on the removal of N-nitrosodimethylamine by polyamide reverse osmosis membranes, Separ. Purif. Technol. 247 (2020) 116921.
[23] S. Shultz, M. Bass, R. Semiat, V. Freger, Modification of polyamide membranes by hydrophobic molecular plugs for improved boron rejection, J. Membr. Sci. 546 (2018) 165–172.
[24] H. Croll, A. Soroush, M.E. Pillsbury, S.R.-V. Castrillón, Graphene oxide surface modification of polyamide reverse osmosis membranes for improved N-nitrosodimethylamine (NDMA) removal, Separ. Purif. Technol. 210 (2019) 973–980.
[25] G.T. Hermanson, in: Chapter 3 the Reactions of Bioconjugation, 2013.
[26] D. Bartczak, A.G. Kanaras, Preparation of peptide-functionalized gold nanoparticles using one pot EDC/Sulfo-NHS coupling, Langmuir 27 (2011) 10119–10123.
[27] C.Y. Tang, Y.-N. Kwon, J.O. Leckie, Effect of membrane chemistry and coating layer on physiochemical properties of thin film composite polyamide RO and NF membranes: I. FTIR and XPS characterization of polyamide and coating layer chemistry, Desalination 242 (2009) 149–167.
[28] E. Nagy, Basic Equations of Mass Transport through a Membrane Layer, Elsevier, 2018.
[29] J. Luo, Y. Wan, Effects of pH and salt on nanofiltration—a critical review, J. Membr. Sci. 438 (2013) 18–28.
[30] D. Chen, J.R. Werber, X. Zhao, M. Elimelech, A facile method to quantify the carboxyl group areal density in the active layer of polyamide thin-film composite membranes, J. Membr. Sci. 534 (2017) 100–108.

Supporting Data

Modification of Polyamide Reverse Osmosis Membranes for the Separation of Urea

Shahriar Habib and Steven T. Weinman*

Department of Chemical and Biological Engineering, The University of Alabama, Tuscaloosa, AL 35487, USA

*Corresponding author: Tel: +1 (205)-348-8516, Fax: +1 (205)-348-7558. Email address: stweinman@eng.ua.edu

Calibration curve for NaCl solution and Urea solution

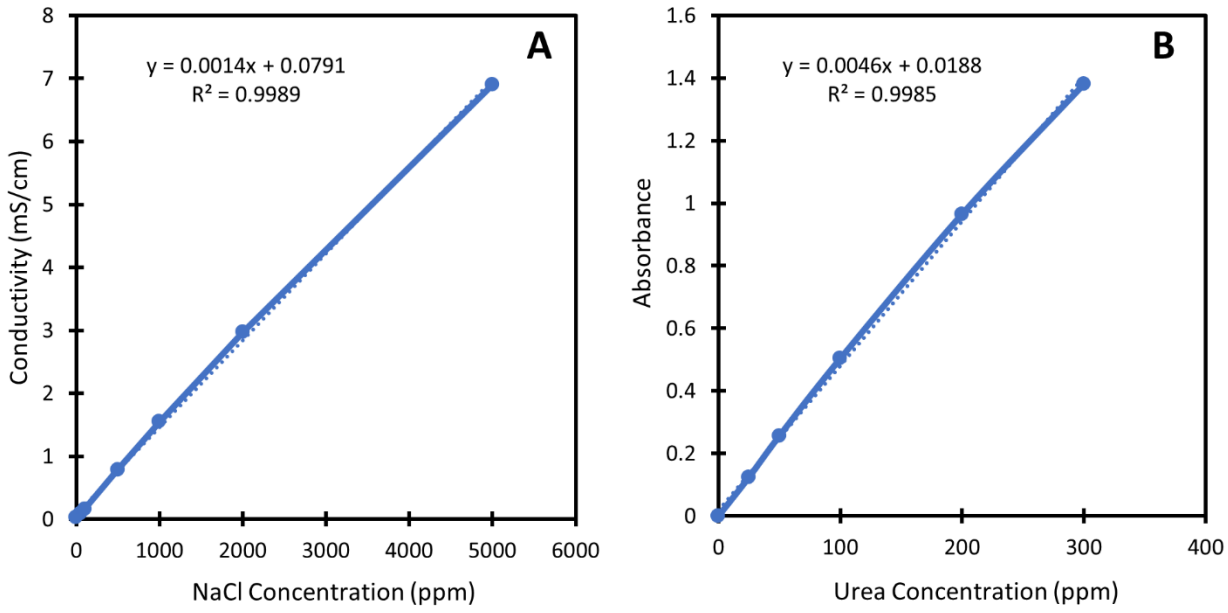

Figure S1. Calibration curve for (A) NaCl solutions and (B) urea solutions in water.

FTIR data for XLE and BW30XFR membranes modified with heat treatment

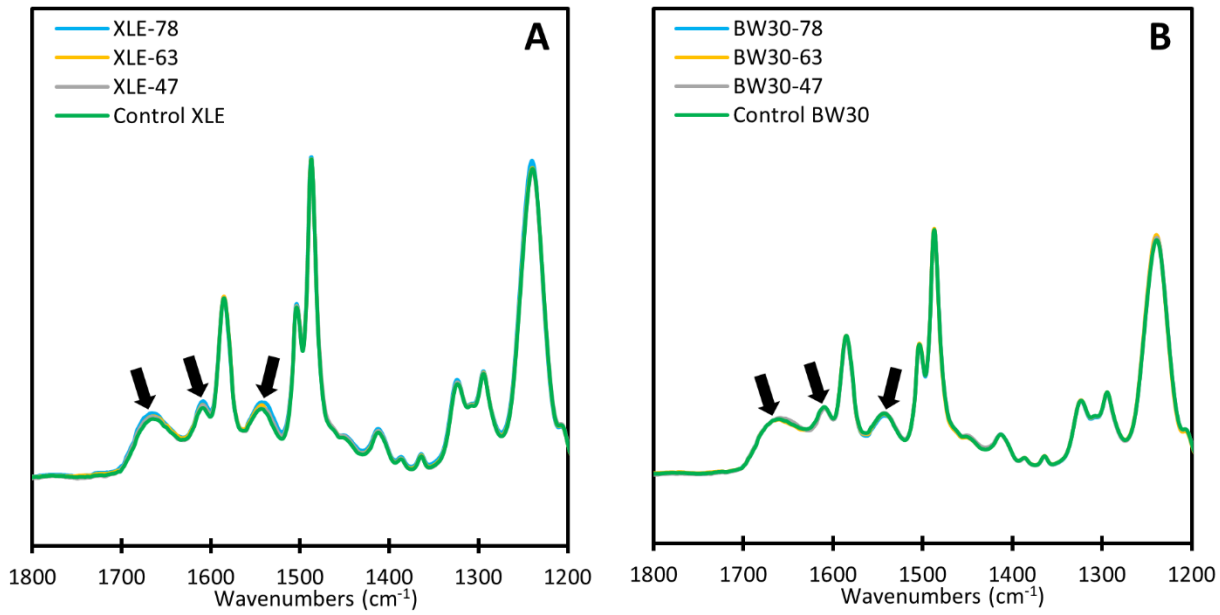

Figure S2. ATR-FTIR spectra of (A) control XLE membrane and XLE membrane modified with 0% MPD at 22 °C, 47 °C, 63 °C, and 78 °C, and (B) control BW30XFR membrane and BW30XFR membrane modified with 0% MPD at 22 °C, 47 °C, 63 °C, and 78 °C.

SEM data for XLE and BW30XFR membranes modified using MPD in post modification

The control and modified XLE and BW30XFR membrane surface morphology were studied using an Apreo field emission scanning electron microscope (FE-SEM, Thermo Fisher Scientific). The membrane samples were dried, attached with carbon tape to aluminum stabs, and sputter-coated with 12 nm of gold (MCM-200 ion sputter coater, SEC Co., Ltd., Korea) prior to SEM imaging. The SEM images were taken at an accelerating voltage of 5 kV, a current voltage of 50 pA, and a magnification of 10,000x.

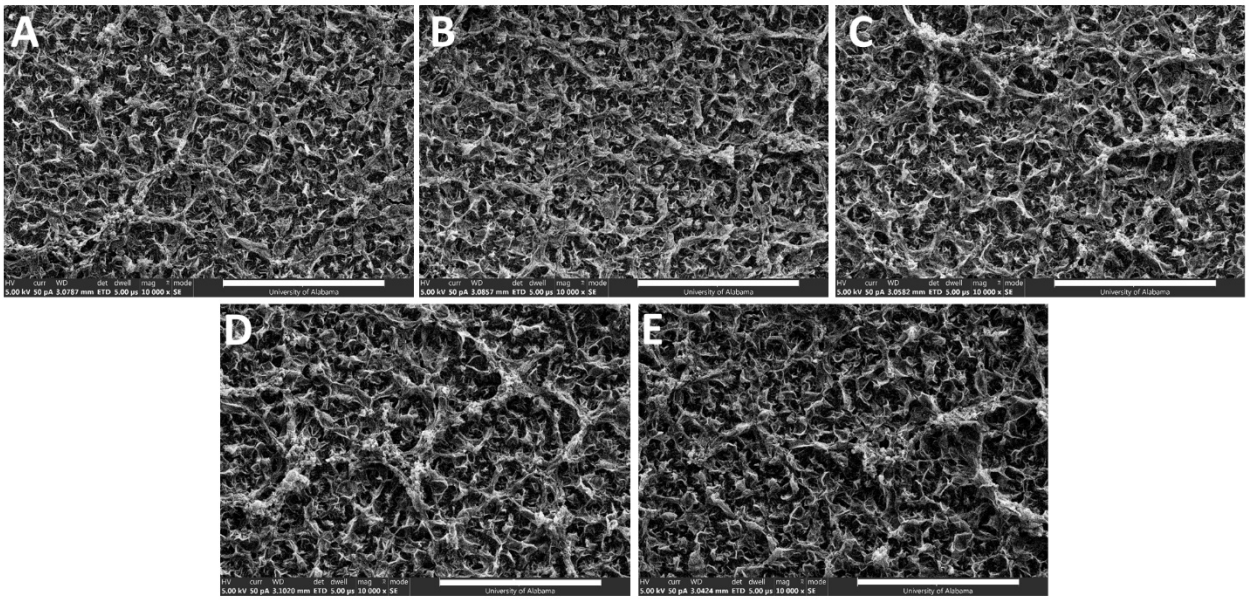

Figure S3. SEM images of (A) control XLE, (B) XLE-NHS-22-MPD, (C) XLE-NHS-47-MPD, (D) XLE-NHS-63-MPD, and (E) XLE-NHS-78-MPD XLE membranes. The white scale bar represents 5 μm.

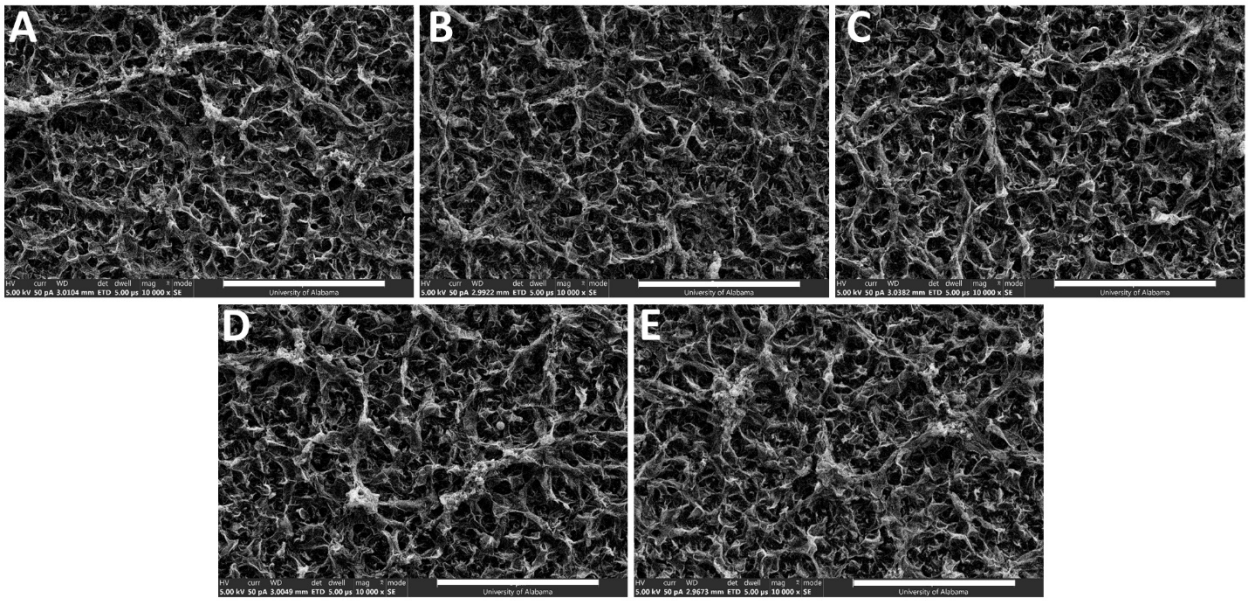

Figure S4. SEM images of (A) control BW30, (B) BW30-NHS-22-MPD, (C) BW30-NHS-47-MPD, (D) BW30-NHS-63-MPD, and (E) BW30-NHS-78-MPD BW30XFR membranes. The white scale bar represents 5 µm.

Zeta Potential data for XLE and BW30XFR membranes modified with heat treatment

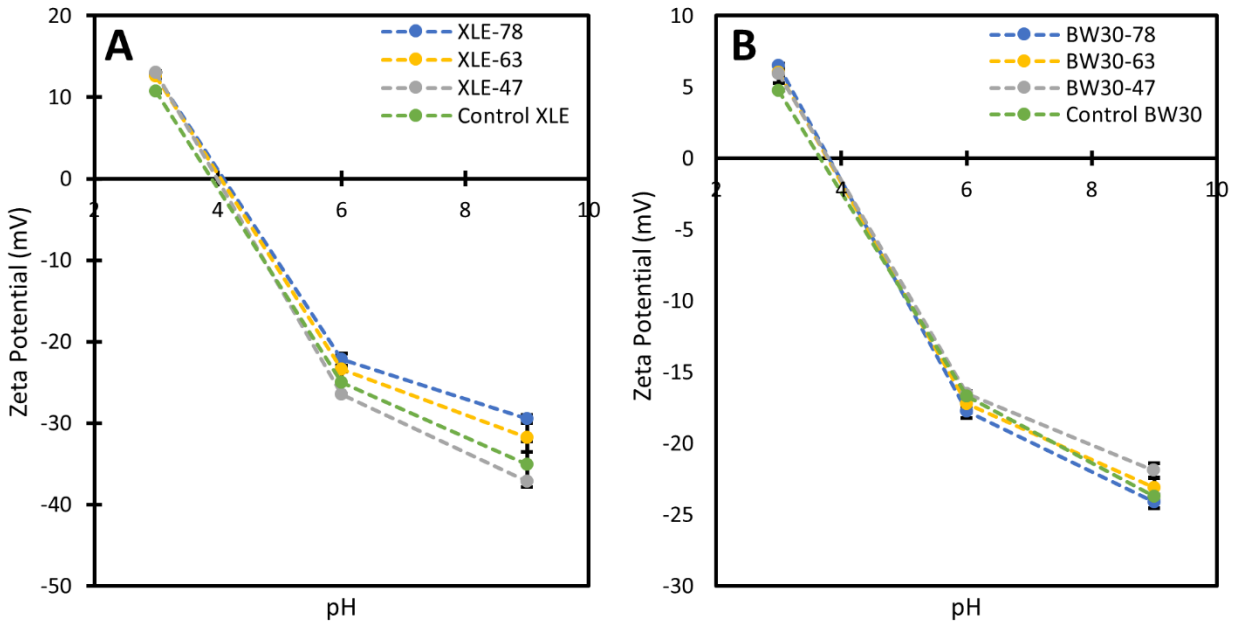

Figure S5. Zeta potential of (A) control XLE membrane and XLE membrane modified with 0% MPD at 22 °C, 47 °C, 63 °C, and 78 °C and (B) control BW30XFR membrane and BW30XFR membrane modified with 0% MPD at 22 °C, 47 °C, 63 °C, and 78 °C at pH 3, pH 6 and pH 9. The error bars represent one standard deviation among three tests. The dashed lines between data points are included to aid in the visual comparison of the different modifications.

Results of Paired t-tests

Results from Paired Two sample t-test for Means Hypothesis testing was done to determine statistical relevance of the data sets. EXCEL (Microsoft O365 Version 1908) was used for all

statistical analyses. All tests were done using 95% confidence ($\alpha = 0.05$); therefore, if the p-value is greater than α then the means are considered to be equal and if the p-value is less than α then the means are considered to be unequal. **Table S1** shows the results from the statistical tests on the N/O ratio from **Table 3** in the main document. **Table S2** shows the results from the statistical tests on the contact angle from **Figure 3** in the main document. **Table S3** shows the results from the statistical tests on the pure water permeance from **Figure 5** in the main document. **Table S4** and **Table S5** show the results from the statistical tests on the water permeance and NaCl rejection data from **Figures 6A and 7A** in the main document for the 2,000 ppm NaCl feed. **Table S6** and **Table S7** show the results from the statistical tests on the water permeance and urea rejection data from **Figures 6B and 7B** in the main document for the 500 ppm urea feed. **Table S8** and **Table S9** show the results from the statistical tests on the NaCl solute permeability and urea solute permeability data from **Figure 8** in the main document.

Table S1. Results of paired t-tests on N/O ratio from XPS measurements.

Group 1 Data	Group 2 Data	Data	Two-tailed P value	Result of Difference
Control XLE	XLE-NHS-22-MPD	N/O Ratio	0.0007	Statistically significant
Control XLE	XLE-NHS-47-MPD	N/O Ratio	0.0045	Statistically significant
Control XLE	XLE-NHS-63-MPD	N/O Ratio	0.0019	Statistically significant
Control XLE	XLE-NHS-78-MPD	N/O Ratio	0.0001	Statistically significant
Control BW30XFR	BW30-NHS-22-MPD	N/O Ratio	0.5682	Not statistically significant
Control BW30XFR	BW30-NHS-47-MPD	N/O Ratio	0.9502	Not statistically significant

Control BW30XFR	BW30-NHS-63-MPD	N/O Ratio	0.0802	Not statistically significant
Control BW30XFR	BW30-NHS-78-MPD	N/O Ratio	0.3166	Not statistically significant

Table S2. Results of paired t-tests on water contact angle measurement.

Group 1 Data	Group 2 Data	Data	Two-tailed P value	Result of Difference
Control XLE	XLE-NHS-22-MPD	Contact Angle	0.0000	Statistically significant
Control XLE	XLE-NHS-47-MPD	Contact Angle	0.0000	Statistically significant
Control XLE	XLE-NHS-63-MPD	Contact Angle	0.0007	Statistically significant
Control XLE	XLE-NHS-78-MPD	Contact Angle	0.0000	Statistically significant
Control XLE	XLE-47	Contact Angle	0.1271	Not statistically significant
Control XLE	XLE-63	Contact Angle	0.0004	Statistically significant
Control XLE	XLE-NHS-78	Contact Angle	0.0060	Statistically significant
XLE-NHS-47-MPD	XLE-47	Contact Angle	0.0000	Statistically significant
XLE-NHS-63-MPD	XLE-63	Contact Angle	0.0003	Statistically significant
XLE-NHS-78-MPD	XLE-78	Contact Angle	0.0000	Statistically significant
Control BW30XFR	BW30-NHS-22-MPD	Contact Angle	0.0115	Statistically significant
Control BW30XFR	BW30-NHS-47-MPD	Contact Angle	0.0030	Statistically significant
Control BW30XFR	BW30-NHS-63-MPD	Contact Angle	0.0002	Statistically significant
Control BW30XFR	BW30-NHS-78-MPD	Contact Angle	0.0000	Statistically significant

Control BW30XFR	BW30-47	Contact Angle	0.0216	Statistically significant
Control BW30XFR	BW30-63	Contact Angle	0.0467	Statistically significant
Control BW30XFR	BW30-78	Contact Angle	0.0007	Statistically significant
BW30-NHS-47-MPD	BW30-47	Contact Angle	0.0005	Statistically significant
BW30-NHS-63-MPD	BW30-63	Contact Angle	0.0062	Statistically significant
BW30-NHS-78-MPD	BW30-78	Contact Angle	0.0000	Statistically significant

66

67 **Table S3.** Results of paired t-tests on pure water permeance.

Group 1 Data	Group 2 Data	Data	Two-tailed P value	Result of Difference
Control XLE	XLE-NHS-22-MPD	Pure Water Permeance	0.0009	Statistically significant
Control XLE	XLE-NHS-47-MPD	Pure Water Permeance	0.0004	Statistically significant
Control XLE	XLE-NHS-63-MPD	Pure Water Permeance	0.0003	Statistically significant
Control XLE	XLE-NHS-78-MPD	Pure Water Permeance	0.0002	Statistically significant
Control XLE	XLE-47	Pure Water Permeance	0.0072	Statistically significant
Control XLE	XLE-63	Pure Water Permeance	0.0015	Statistically significant
Control XLE	XLE-78	Pure Water Permeance	0.0008	Statistically significant
XLE-NHS-47-MPD	XLE-47	Pure Water Permeance	0.0000	Statistically significant
XLE-NHS-63-MPD	XLE-63	Pure Water Permeance	0.0261	Statistically significant
XLE-NHS-78-MPD	XLE-78	Pure Water Permeance	0.0007	Statistically significant

Control BW30XFR	BW30-NHS-22-MPD	Pure Water Permeance	0.0000	Statistically significant
Control BW30XFR	BW30-NHS-47-MPD	Pure Water Permeance	0.0000	Statistically significant
Control BW30XFR	BW30-NHS-63-MPD	Pure Water Permeance	0.0002	Statistically significant
Control BW30XFR	BW30-NHS-78-MPD	Pure Water Permeance	0.0001	Statistically significant
Control BW30XFR	BW30-47	Pure Water Permeance	0.0002	Statistically significant
Control BW30XFR	BW30-63	Pure Water Permeance	0.0019	Statistically significant
Control BW30XFR	BW30-78	Pure Water Permeance	0.0000	Statistically significant
BW30-NHS-47-MPD	BW30-47	Pure Water Permeance	0.9209	Not statistically significant
BW30-NHS-63-MPD	BW30-63	Pure Water Permeance	0.0078	Statistically significant
BW30-NHS-78-MPD	BW30-78	Pure Water Permeance	0.0084	Statistically significant

Table S4. Results of paired t-tests on water permeance during the NaCl rejection tests for the XLE and BW30XFR membranes.

Group 1 Data	Group 2 Data	Data	Two-tailed P value	Result of Difference
Control XLE	XLE-NHS-22-MPD	Water Permeance	0.0016	Statistically significant
Control XLE	XLE-NHS-47-MPD	Water Permeance	0.0004	Statistically significant
Control XLE	XLE-NHS-63-MPD	Water Permeance	0.0002	Statistically significant
Control XLE	XLE-NHS-78-MPD	Water Permeance	0.0001	Statistically significant
Control XLE	XLE-47	Water Permeance	0.0036	Statistically significant

Control XLE	XLE-63	Water Permeance	0.0009	Statistically significant
Control XLE	XLE-78	Water Permeance	0.0003	Statistically significant
XLE-NHS-47-MPD	XLE-47	Water Permeance	0.0010	Statistically significant
XLE-NHS-63-MPD	XLE-63	Water Permeance	0.0020	Statistically significant
XLE-NHS-78-MPD	XLE-78	Water Permeance	0.0012	Statistically significant
Control BW30XFR	BW30-NHS-22-MPD	Water Permeance	0.0011	Statistically significant
Control BW30XFR	BW30-NHS-47-MPD	Water Permeance	0.0002	Statistically significant
Control BW30XFR	BW30-NHS-63-MPD	Water Permeance	0.0002	Statistically significant
Control BW30XFR	BW30-NHS-78-MPD	Water Permeance	0.0001	Statistically significant
Control BW30XFR	BW30-47	Water Permeance	0.0000	Statistically significant
Control BW30XFR	BW30-63	Water Permeance	0.0001	Statistically significant
Control BW30XFR	BW30-78	Water Permeance	0.0000	Statistically significant
BW30-NHS-47-MPD	BW30-47	Water Permeance	0.1179	Not statistically significant
BW30-NHS-63-MPD	BW30-63	Water Permeance	0.0024	Statistically significant
BW30-NHS-78-MPD	BW30-78	Water Permeance	0.0101	Statistically significant

71

72 **Table S5.** Results of paired t-tests on NaCl rejection for the XLE and BW30XFR membranes.

Group 1 Data	Group 2 Data	Data	Two-tailed P value	Result of Difference
Control XLE	XLE-NHS-22-MPD	NaCl Rejection	0.4211	Not statistically significant

Control XLE	XLE-NHS-47-MPD	NaCl Rejection	0.1249	Not statistically significant
Control XLE	XLE-NHS-63-MPD	NaCl Rejection	0.1536	Not statistically significant
Control XLE	XLE-NHS-78-MPD	NaCl Rejection	0.0320	Statistically significant
Control XLE	XLE-47	NaCl Rejection	0.5918	Not statistically significant
Control XLE	XLE-63	NaCl Rejection	0.1649	Not statistically significant
Control XLE	XLE-78	NaCl Rejection	0.8202	Not statistically significant
XLE-NHS-47-MPD	XLE-47	NaCl Rejection	0.2925	Not statistically significant
XLE-NHS-63-MPD	XLE-63	NaCl Rejection	0.0024	Statistically significant
XLE-NHS-78-MPD	XLE-78	NaCl Rejection	0.0224	Statistically significant
Control BW30XFR	BW30-NHS-22-MPD	NaCl Rejection	0.3352	Not statistically significant
Control BW30XFR	BW30-NHS-47-MPD	NaCl Rejection	0.3710	Not statistically significant
Control BW30XFR	BW30-NHS-63-MPD	NaCl Rejection	0.0277	Statistically significant
Control BW30XFR	BW30-NHS-78-MPD	NaCl Rejection	0.0194	Statistically significant
Control BW30XFR	BW30-47	NaCl Rejection	0.7948	Not statistically significant
Control BW30XFR	BW30-63	NaCl Rejection	0.8225	Not statistically significant
Control BW30XFR	BW30-78	NaCl Rejection	0.8723	Not statistically significant
BW30-NHS-47-MPD	BW30-47	NaCl Rejection	0.1261	Not statistically significant
BW30-NHS-63-MPD	BW30-63	NaCl Rejection	0.0103	Statistically significant

BW30-NHS-78-MPD	BW30-78	NaCl Rejection	0.0028	Statistically significant

Table S6. Results of paired t-tests on water permeance during the urea rejection tests for the XLE and BW30XFR membranes.

Group 1 Data	Group 2 Data	Data	Two-tailed P value	Result of Difference
Control XLE	XLE-NHS-22-MPD	Water Permeance	0.0004	Statistically significant
Control XLE	XLE-NHS-47-MPD	Water Permeance	0.0004	Statistically significant
Control XLE	XLE-NHS-63-MPD	Water Permeance	0.0001	Statistically significant
Control XLE	XLE-NHS-78-MPD	Water Permeance	0.0001	Statistically significant
Control XLE	XLE-47	Water Permeance	0.0009	Statistically significant
Control XLE	XLE-63	Water Permeance	0.0004	Statistically significant
Control XLE	XLE-78	Water Permeance	0.0002	Statistically significant
XLE-NHS-47-MPD	XLE-47	Water Permeance	0.0093	Statistically significant
XLE-NHS-63-MPD	XLE-63	Water Permeance	0.0017	Statistically significant
XLE-NHS-78-MPD	XLE-78	Water Permeance	0.0015	Statistically significant
Control BW30XFR	BW30-NHS-22-MPD	Water Permeance	0.0004	Statistically significant
Control BW30XFR	BW30-NHS-47-MPD	Water Permeance	0.0002	Statistically significant
Control BW30XFR	BW30-NHS-63-MPD	Water Permeance	0.0001	Statistically significant
Control BW30XFR	BW30-NHS-78-MPD	Water Permeance	0.0001	Statistically significant

Control BW30XFR	BW30-47	Water Permeance	0.0000	Statistically significant
Control BW30XFR	BW30-63	Water Permeance	0.0009	Statistically significant
Control BW30XFR	BW30-78	Water Permeance	0.000	Statistically significant
BW30-NHS-47-MPD	BW30-47	Water Permeance	0.1308	Not statistically significant
BW30-NHS-63-MPD	BW30-63	Water Permeance	0.0053	Statistically significant
BW30-NHS-78-MPD	BW30-78	Water Permeance	0.0121	Statistically significant

Table S7. Results of paired t-tests on urea rejection for the XLE and BW30XFR membranes.

Group 1 Data	Group 2 Data	Data	Two-tailed P value	Result of Difference
Control XLE	XLE-NHS-22-MPD	Urea Rejection	0.0000	Statistically significant
Control XLE	XLE-NHS-47-MPD	Urea Rejection	0.0000	Statistically significant
Control XLE	XLE-NHS-63-MPD	Urea Rejection	0.0000	Statistically significant
Control XLE	XLE-NHS-78-MPD	Urea Rejection	0.0000	Statistically significant
Control XLE	XLE-47	Urea Rejection	0.0000	Statistically significant
Control XLE	XLE-63	Urea Rejection	0.0000	Statistically significant
Control XLE	XLE-78	Urea Rejection	0.0000	Statistically significant
XLE-NHS-47-MPD	XLE-47	Urea Rejection	0.0000	Statistically significant
XLE-NHS-63-MPD	XLE-63	Urea Rejection	0.0007	Statistically significant
XLE-NHS-78-MPD	XLE-78	Urea Rejection	0.0396	Statistically significant

Control BW30XFR	BW30-NHS-22-MPD	Urea Rejection	0.0079	Statistically significant
Control BW30XFR	BW30-NHS-47-MPD	Urea Rejection	0.0032	Statistically significant
Control BW30XFR	BW30-NHS-63-MPD	Urea Rejection	0.0005	Statistically significant
Control BW30XFR	BW30-NHS-78-MPD	Urea Rejection	0.0004	Statistically significant
Control BW30XFR	BW30-47	Urea Rejection	0.0018	Statistically significant
Control BW30XFR	BW30-63	Urea Rejection	0.0001	Statistically significant
Control BW30XFR	BW30-78	Urea Rejection	0.0018	Statistically significant
BW30-NHS-47-MPD	BW30-47	Urea Rejection	0.5736	Not statistically significant
BW30-NHS-63-MPD	BW30-63	Urea Rejection	0.1050	Not statistically significant
BW30-NHS-78-MPD	BW30-78	Urea Rejection	0.1422	Not statistically significant

Table S8. Results of paired t-tests on NaCl solute permeability for the XLE and BW30XFR membranes.

Group 1 Data	Group 2 Data	Data	Two-tailed P value	Result of Difference
Control XLE	XLE-NHS-22-MPD	NaCl permeability	0.2197	Not statistically significant
Control XLE	XLE-NHS-47-MPD	NaCl permeability	0.0133	Statistically significant
Control XLE	XLE-NHS-63-MPD	NaCl permeability	0.0210	Statistically significant
Control XLE	XLE-NHS-78-MPD	NaCl permeability	0.0366	Statistically significant
Control XLE	XLE-47	NaCl permeability	0.0702	Not statistically significant

Control XLE	XLE-63	NaCl permeability	0.0159	Statistically significant
Control XLE	XLE-78	NaCl permeability	0.0156	Statistically significant
XLE-NHS-47-MPD	XLE-47	NaCl permeability	0.1448	Not statistically significant
XLE-NHS-63-MPD	XLE-63	NaCl permeability	0.2730	Not statistically significant
XLE-NHS-78-MPD	XLE-78	NaCl permeability	0.8049	Statistically significant
Control BW30XFR	BW30-NHS-22-MPD	NaCl permeability	0.2296	Not statistically significant
Control BW30XFR	BW30-NHS-47-MPD	NaCl permeability	0.1913	Not statistically significant
Control BW30XFR	BW30-NHS-63-MPD	NaCl permeability	0.3624	Not statistically significant
Control BW30XFR	BW30-NHS-78-MPD	NaCl permeability	0.9911	Not statistically significant
Control BW30XFR	BW30-47	NaCl permeability	0.3847	Not statistically significant
Control BW30XFR	BW30-63	NaCl permeability	0.3195	Not statistically significant
Control BW30XFR	BW30-78	NaCl permeability	0.2432	Not statistically significant
BW30-NHS-47-MPD	BW30-47	NaCl permeability	0.1328	Not statistically significant
BW30-NHS-63-MPD	BW30-63	NaCl permeability	0.9167	Not statistically significant
BW30-NHS-78-MPD	BW30-78	NaCl permeability	0.0275	Statistically significant

Table S9. Results of paired t-tests on urea solute permeability for the XLE and BW30XFR membranes.

Group 1 Data	Group 2 Data	Data	Two-tailed P value	Result of Difference

Control XLE	XLE-NHS-22-MPD	Urea permeability	0.0005	Statistically significant
Control XLE	XLE-NHS-47-MPD	Urea permeability	0.0002	Statistically significant
Control XLE	XLE-NHS-63-MPD	Urea permeability	0.0000	Statistically significant
Control XLE	XLE-NHS-78-MPD	Urea permeability	0.0000	Statistically significant
Control XLE	XLE-47	Urea permeability	0.0004	Statistically significant
Control XLE	XLE-63	Urea permeability	0.0002	Statistically significant
Control XLE	XLE-78	Urea permeability	0.0001	Statistically significant
XLE-NHS-47-MPD	XLE-47	Urea permeability	0.0020	Statistically significant
XLE-NHS-63-MPD	XLE-63	Urea permeability	0.0019	Statistically significant
XLE-NHS-78-MPD	XLE-78	Urea permeability	0.0017	Statistically significant
Control BW30XFR	BW30-NHS-22-MPD	Urea permeability	0.0000	Statistically significant
Control BW30XFR	BW30-NHS-47-MPD	Urea permeability	0.0000	Statistically significant
Control BW30XFR	BW30-NHS-63-MPD	Urea permeability	0.0000	Statistically significant
Control BW30XFR	BW30-NHS-78-MPD	Urea permeability	0.0000	Statistically significant
Control BW30XFR	BW30-47	Urea permeability	0.0000	Statistically significant
Control BW30XFR	BW30-63	Urea permeability	0.0001	Statistically significant
Control BW30XFR	BW30-78	Urea permeability	0.0000	Statistically significant
BW30-NHS-47-MPD	BW30-47	NaCl permeability	0.1136	Not statistically significant

BW30-NHS-63-MPD	BW30-63	NaCl permeability	0.00160	Statistically significant
BW30-NHS-78-MPD	BW30-78	NaCl permeability	0.0399	Statistically significant

84